Earth and Planetary Science Letters 430 (2015) 140–148

Contents lists available at ScienceDirect

Earth and Planetary Science Letters

www.elsevier.com/locate/epsl

Seismic imaging of deep crustal melt sills beneath Costa Rica suggests a method for the formation of the Archean continental crust

Nicholas Harmon [*], Catherine A. Rychert

University of Southampton, Ocean and Earth Science, National Oceanography Centre, European Way, Southampton, SO143ZH, United Kingdom

ARTICLE INFO

Article history:
Received 26 January 2015
Received in revised form 24 July 2015
Accepted 28 July 2015
Available online 28 August 2015
Editor: J. Brodholt

Keywords:
surface waves
tomography
seismic anisotropy
continental crust
oceanic crust
subduction zones

ABSTRACT

Continental crust formed billions of years ago but cannot be explained by a simple evolution of primary mantle magmas. A multi-step process is required that likely includes re-melting of wet metamorphosed basalt at high pressures. Such a process could occur at depth in oceanic crust that has been thickened by a large magmatic event. In Central America, variations in geologically inferred, pre-existing oceanic crustal thickness beneath the arc provides an excellent opportunity to study its effect on magma storage, re-melting of meta-basalts, and the potential for creating continental crust. We use surface waves derived from ambient noise tomography to image 6% radially anisotropic structures in the thickened oceanic plateau crust of Costa Rica that likely represent deep crustal melt sills. In Nicaragua, where the arc is forming on thinner oceanic crust, we do not image these deep crustal melt sills. The presence of these deep sills correlates with more felsic arc outputs from the Costa Rican Arc suggesting pre-existing thickened crust accelerates processing of primary basalts to continental compositions. In the Archean, reprocessing thickened oceanic crust by subsequent hydrated hotspot volcanism or subduction zone volcanism may have similarly enhanced formation of early continental crust. This mechanism may have been particularly important if subduction did not initiate until 3 Ga.

1. Introduction

The Central American Arc presents a unique opportunity to examine the role of crustal thickness in magmatic differentiation and continent formation due to the juxtaposition of thick oceanic crust in Costa Rica and thinner oceanic crust in Nicaragua. The Costa Rican Arc is forming on oceanic lithosphere formed from the Caribbean Large Igneous Province, which is thought to be related to the Galapagos Plume (Hauff et al., 2000), with crustal thicknesses up to 40 km (Linkimer et al., 2010; MacKenzie et al., 2008). In contrast, the arc in Nicaragua currently lies on thinned crust that varies from 20–30 km across the region (MacKenzie et al., 2008) of possibly oceanic origins of an accreted terrane (Baumgartner et al., 2008; Venable, 1994) with a continental crustal block to the North (Dengo, 1985). In addition, the Nicaraguan and Costa Rican Arcs produce basaltic and silicic magmas (Vogel et al., 2004, 2006) that appear to have little crustal assimilation (Carr et al., 2003), suggesting that differentiation of primary magmas is active in both segments of the arc. Imaging the crustal structure provides insights into magmatic differentiation processes through a better understanding of magma storage depths and structure associated with magma plumbing.

In this paper we present a new radially anisotropic shear velocity model for Costa Rica and Nicaragua. Our findings illuminate the role of crustal thickness in transforming oceanic crust into continental crust. The results are then related to a conceptual model for early continental crust formation.

2. Methods

We used 18 months of continuous three component data (vertical, north and east) from the Tomography Under Costa Rica and Nicaragua (TUCAN) seismic array to calculate noise cross correlation functions (NCF) to estimate short period surface wave dispersion (Fig. 1). To preprocess the data, we removed the instrument response, decimated to 1 Hz, and band pass filtered between 0.01–0.30 Hz. We calculated noise cross correlation functions on daylong seismograms between all possible station pairs and components after the method of Bensen et al. (2007). To normalize the data to reduce the effects of earthquakes we used the average of all three components with a moving average window of 100 s. The radial and transverse components for each station pair were determined after stacking by rotation (Lin et al., 2008). This type of processing has been successfully applied to extract Love wave in-

---

[*] Corresponding author.
E-mail address: n.harmon@soton.ac.uk (N. Harmon).

http://dx.doi.org/10.1016/j.epsl.2015.07.062
0012-821X/© 2015 Elsevier B.V. All rights reserved.

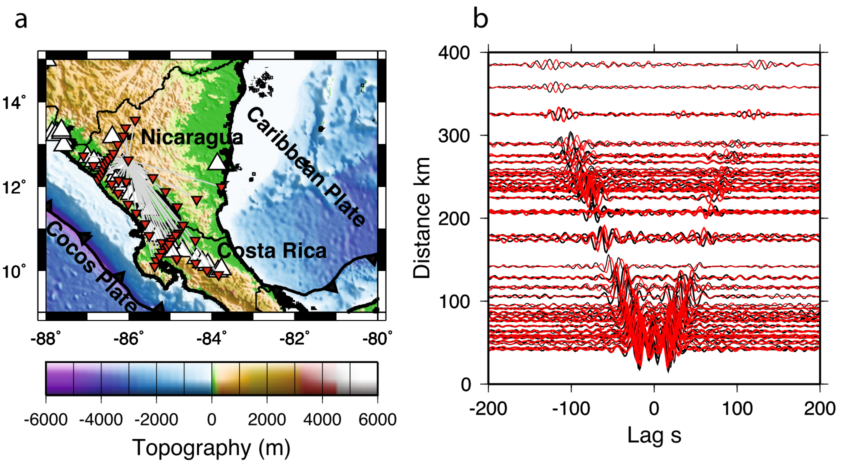

Fig. 1. Station and location map (a), NCF for selected station paths. (b) Station locations (red triangles), active volcanoes (white triangles) and major features are indicated in (a). NCF for transverse–transverse component (red) and vertical–vertical components (black) in (b). (For interpretation of the references to color in this figure legend, the reader is referred to the web version of this article.)

formation (e.g. Lin et al., 2008) and follows on from the theory for scalar wave equation noise cross correlation (Sanchez-Sesma and Campillo, 2006).

Our tomography is a three-step process. In the first step, the average dispersion curve for the region is determined, initially through beamforming, then using the average of all useable station-to-station pairs at each period. Then phase velocity maps are estimated through tomographic inversion using the average phase velocity at each period as the starting model. Then we invert our average dispersion curves for Rayleigh and Love waves for the best fitting radially anisotropic shear velocity as well as the radially anisotropic shear velocity for each location of the phase velocity maps to generate a 3-D velocity structure for the region.

To verify the noise distribution was sufficient for tomography we used a beamforming technique (Harmon et al., 2008, 2010), which correlates the NCF with plane wave sources over a range of horizontal slowness and back azimuths for both the vertical and horizontal components. To determine the transverse beamformer output, the data were rotated to each back azimuth tested. The beamforming also provided a starting average phase velocity for the region for Love waves by determining the best fitting average slowness at each period of interest.

Phase velocities for each station pair were determined after Harmon et al. (2007). In the method, the fundamental mode Rayleigh and Love waves are windowed from the symmetric component of the vertical-to-vertical and transverse-to-transverse components of the NCF respectively. We Fourier transformed the records, and determined the unwrapped phase. The phase was corrected for the $\pi/4$ phase shift due to the cross correlation (Harmon et al., 2007), and the cycle ambiguity resolved by matching the phase velocity of each NCF at the longest periods (25 s) to the average phase velocity determined by beamforming in the case of Love waves and a previous teleseismic and ambient noise study for Rayleigh waves (Harmon et al., 2013). We tested to confirm that Love waves require the same $\pi/4$ phase shift correction applied to Rayleigh waves to match the phase velocities determined from beamforming (Harmon et al., 2008). We generated phase velocity maps after Harmon et al. (2013), and for each period >200 phase measurements were used after signal-to-noise (SNR >3), station-to-station distance (>3 x wavelength) and error (within ± 0.2 km/s of average velocity) criteria were met. We define SNR as the amplitude of the Love or Rayleigh wave at a given period compared with the root mean square amplitude of a 60 s window of noise at lag times 700–760 s in the NCF. We also used the same nodal parameterization as Harmon et al. (2013), with a 0.25° spacing in latitude and longitude. We used 2-D sensitivity kernels (Nishida, 2011; Zhou et al., 2004) in our tomographic inversion, as it has been shown that the sensitivity for a uniform noise distribution is nearly identical to phase velocity kernels used in traditional earthquake tomography (Nishida, 2011; Tromp et al., 2010). We evaluate the noise source distribution and the use of the sensitivity kernels in the Section 2.1.

In the phase velocity maps for the Love wave inversions, the diagonals of the formal resolution matrix have maximum values of 0.44 at our best resolved period 10 s (Fig. 2). This resolution is derived from the sensitivity kernels centered nominally on the ray paths shown in Fig. 2 for 10, 15, 20 s period. Thus, formal resolution indicates that an average of two to three nodes produces an independent piece of information about the velocity structure. In other words velocity variations at <2 node spacing length scale are not resolved, so we limit our discussion to features at >60 km wavelength.

We model radially anisotropic shear velocity from our phase velocity maps and 1-D dispersion curve using density, ρ, and five elastic parameters, $\mathrm{A} = \rho\alpha_{\mathrm{H}}^2$, $\mathrm{C} = \rho\alpha_{\mathrm{V}}^2$, $\mathrm{L} = \rho\beta_{\mathrm{V}}^2$, $\mathrm{N} = \rho\beta_{\mathrm{H}}^2$, and F (Montagner and Anderson, 1989), where α is compressional velocity and β is shear velocity, and subscript H and V denote horizontal and vertical respectively. We use an alternative parameterization, $\xi = \mathrm{N}/\mathrm{L}$, $\phi = \mathrm{C}/\mathrm{A}$, $\eta = \mathrm{F}/(\mathrm{A} - 2\mathrm{L})$, β_{V}, and α_{H} for the elastic parameters (Saito, 1988). Typically only two out of the five parameters can be well resolved, β_{V} and ξ, so to reduce the number of parameters we scale $\delta \ln \phi = -1.5 \ln \xi$, $\delta \ln \eta = -2.5 \ln \xi$ (Montagner and Anderson, 1989; Panning and Romanowicz, 2006). We fix the α/β ratio to 1.80 in the mantle and use the α/β ratios in the crust from receiver function studies in the region, interpolated between stations (Linkimer et al., 2010; MacKenzie et al., 2008). As the scaling factors are appropriate for a mantle peridotite, we tested the effect of our choice of scaling factors and α/β ratio on our final results for the 1-D inversion. Variation in our scaling factors by up to ± 1.0, resulted in $<1\%$ variation in our result. The anisotropy in our model is required for α/β ratios >1.65, i.e., typical crustal ranges.

We use an Occam inversion scheme (Constable et al., 1987) for vertically polarized shear velocity (β_{V}) and ξ, using sensitivity kernels calculated using DISPER80 (Saito, 1988). We use 2 km thick layers in the upper 50 km, transitioning to 50 km layer thickness at 150 km depth to 600 km depth. The inversion scheme balances model smoothness vs fit by searching over a range of smoothing factors. For our starting model we use the best fit average shear velocity model from previous work using Rayleigh waves